Effects of Growth Factor Combinations TGFβ3, GDF5 and GDF6 on the Matrix Synthesis of Nucleus Pulposus and Nasoseptal Chondrocyte Self-Assembled Microtissues

Shani Samuel [1,2], Emily E. McDonnell [1,2] and Conor T. Buckley [1,2,3,4,*]

[1] Trinity Centre for Biomedical Engineering, Trinity Biomedical Sciences Institute, Trinity College Dublin, The University of Dublin, Dublin, D02 R590, Ireland; samuelsh@tcd.ie (S.S.), mcdonne5@tcd.ie (E.E.M.)

[2] Discipline of Mechanical, Manufacturing and Biomedical Engineering, School of Engineering, Trinity College Dublin, The University of Dublin, Dublin, D02 PN40, Ireland

[3] Advanced Materials and Bioengineering Research (AMBER) Centre, Royal College of Surgeons in Ireland & Trinity College Dublin, The University of Dublin, Dublin, D02 PN40, Ireland

[4] Tissue Engineering Research Group, Department of Anatomy and Regenerative Medicine, Royal College of Surgeons in Ireland, 121/122 St. Stephen's Green, Dublin, D02 H903, Ireland

* Correspondence: conor.buckley@tcd.ie

Abstract: There has been significant interest in identifying alternative cell sources and growth factor stimulation to improve matrix synthesis for disc repair. Recent work has identified nasoseptal chondrocytes (NC) as a possible alternative cell source with significant matrix-forming abilities. While various growth factors such as members of the TGFβ superfamily have been explored to enhance matrix formation, no consensus exists as to the optimum growth factor needed to induce cells towards a discogenic phenotype. This study assessed both nucleus pulposus (NP) and NC microtissues of different densities (1000, 2500 or 5000 cells/microtissue) stimulated by individual or combinations of the growth factors TGFβ3, GDF5, and GDF6. Lower cell densities result in increased sGAG/DNA and collagen/DNA levels due to higher nutrient availability levels. Our findings suggest that growth factors exert differential effects on matrix synthesis depending on the cell type. NP cells were found to be relatively insensitive to the different growth factor types examined in isolation or in combination. Overall, NCs exhibited a higher propensity to form extracellular matrix compared to NP cells. In addition, stimulating NC-microtissues with GDF5 or TGFβ3 alone induced enhanced matrix formation and may be an appropriate growth factor to stimulate this cell type for disc regeneration.

Keywords: microwell; GFD5; GDF6; TGFβ3; microtissues; intervertebral disc

1. Introduction

Cell-based therapies may hold significant potential as a treatment strategy for the repair and regeneration of the intervertebral disc (IVD). However, it remains challenging to identify an appropriate cell source that can be obtained with minimal donor site morbidity and produce a matrix with high levels of proteoglycan containing predominately collagen type II and low levels of collagen type I. The most commonly explored cell types for IVD regeneration include mesenchymal stem cells (MSCs) [1,2], articular chondrocytes [3] and disc-derived cells [4]. Studies have demonstrated that reimplantation of extracted NP cells can retard degenerative changes, and the injection of autologous nucleus pulposus (NP) cells has been clinically tested in humans with positive outcomes [5]. DiscGenics Inc. (Salt Lake City, Utah) is actively investigating their propriety technology IDCT (injectable discogenic cell therapy) which contains a mixture of progenitor cells derived from allogeneic "discogenic" cells and a viscous biomaterial [6]. However, the use of NP cells is limited due to the matrix-forming capacity of expanded NP cells derived from degenerated tissue [7] and the number of nucleus pulposus (NP) cells that can be isolated from a degenerated disc is insufficient [8] to meet the requirements for successful treatment without significant culture expansion.

In contrast, stem cells can be obtained from various sources (bone marrow or adipose tissue) and have been shown to survive and proliferate after implantation into the disc [9]. However, cell leakage at the injection site has been shown to result in osteophyte formation [10]. Mature chondrocytes produce a matrix similar to NP cells with nasoseptal chondrocytes (NCs) being recently explored as an alternative non-disc cell source for IVD regeneration. NCs have a higher cell yield and sulphated glycosaminoglycan (sGAG) synthesis [11] when compared to articular chondrocytes (ACs) and MSCs [12]. Recently, Borrelli et al. also demonstrated that NCs resulted in higher matrix synthesis levels in comparison to NP cells [13]. The use of NCs for IVD regeneration may present many advantages compared to NP cells, including a high cell yield [11], the ability to produce tissue in an age-independent manner [14,15], enhanced matrix synthesis [13] and can be obtained with minimal donor site morbidity facilitating their autologous use. These intrinsic properties make NCs an attractive non-disc cell source for IVD regeneration.

Growth factors regulate IVD homeostasis, including extracellular matrix (ECM) synthesis and degradation, cell differentiation, or apoptosis [16]. Researchers have widely investigated the potential of various growth factor-mediated induction of cells to mimic the expression profile resembling native disc tissue. Studies have shown that the activation of transforming growth factor beta (TGFβ) signalling pathways delays IVD degeneration by increasing ECM

synthesis [17,18] and hence members of the TGFβ superfamily may be potential candidates for driving discogenic differentiation and phenotype. TGFβ3 has been shown to maintain the phenotype of disc cells in organ culture [19] and when encapsulated with MSCs, they induced IVD regeneration in vivo [20]. Growth differentiation factor 5 (GDF5) and GDF6 are members of the bone morphogenetic protein (BMP) family. GDF5 and GDF6 play important roles in the development of bones, limb joints, skull and axial skeleton [21] and are also expressed in developing cartilage, tendons and ligaments [22,23]. In GDF5/6-knockout mouse models, the vertebral column showed severe lateral curvature and reduced staining of the IVDs indicating lower proteoglycan content [22]. These results suggest that GDF5 and GDF6 are required for normal development and maintenance of the IVD. In pellet culture, GDF5 results in reduced expression of the catabolic enzyme MMP13 in human chondrocytes [24]. There is also evidence to suggest that GDF-5 confers protection against NP cell apoptosis, promotes the synthesis of the main components of the extracellular matrix and can inhibit the activation of the NF-κB signalling pathway, thereby down-regulating the expression of inflammatory cytokines [25]. Inflammatory cytokines play an important role in the pathogenesis of disc degeneration by promoting matrix breakdown and recruitment of immune cells [26]. GDF6 supplementation has been shown to increase both proteoglycan and collagen production in 3D alginate bead cultures of human NP and AF cells [27]. Clarke et al. previously tested the individual effects of TGFβ3, GDF5, and GDF6 on discogenesis of bone marrow-derived MSCs and adipose-derived stem cells (ADSCs) reporting that GDF6 induced differentiation of these cell types towards an NP-like phenotype to a greater extent compared to other growth factors [28]. Furthermore, the authors found optimal expression of genes COL2 and ACAN when stimulated with 10 ng/mL TGFβ3 and 100 ng/mL GDF5 and GDF6. However, they did not investigate the effect of combining these growth factors. The overall objective of this study was to assess and compare the extent of matrix deposited by NP and NC microtissues stimulated by individual or combinations of the growth factors TGFβ3, GDF5, and GDF6.

2. Materials and Methods

2.1. Nucleus Pulposus and Nasoseptal Chondrocyte Isolation and Expansion

All tissue was sourced from a local abattoir and dissected within 24 h. NP cells were isolated from the IVDs of porcine spines (3 female donors; 4 months old). Briefly, NP tissues were harvested aseptically from the central nucleus pulposus of the IVD avoiding the annulus fibrosus region, washed with phosphate-buffered saline (PBS) and minced. Tissue fragments were placed in T-25 flasks containing Low Glucose-Dulbecco's Modified Eagle Medium (LG-DMEM) with 10% foetal bovine serum (FBS) and penicillin (100 U/mL)-streptomycin (100 μg/mL) (PenStrep) and cultured in a humidified atmosphere at 37 °C and 5 %CO_2. After ~7 days, cells had migrated from the tissue fragments, the flasks were washed with PBS and the cells were expanded to 80% confluence. NCs were isolated from porcine nasal septa, washed with PBS and minced. To isolate NC cells, minced tissue was digested in serum free LG-DMEM containing PenStrep and 3000 U/mL collagenase type II (Gibco, Invitrogen, Ireland) at a ratio of 10 mL/g of minced tissue. Digestion was performed under constant rotation for 3 h at 37 °C and subjected to physical agitation using a tissue dissociator (GentleMACS™, Miltenyi Biotech, Surrey, UK) as previously described [29]. Digested tissue/cell suspensions were passed through a 40 μm cell strainer to remove tissue debris. Cell yield and viability in both cases were determined with a hemocytometer and trypan blue exclusion. Cells were seeded at an initial density of 5×10^3 cells/cm^2 in T-175 flasks in LG-DMEM supplemented with 10% FBS and PenStrep. Cultures were expanded to passage two in a humidified atmosphere at 37 °C and 5 %CO_2.

2.2. Fabrication of PDMS Microwell Moulds and Microtissue Formation

Concave PDMS (polydimethylsiloxane) microwells were employed to generate self-assembled microtissues using lower numbers of cells than traditional pellet cultures or alginate bead models using a similar approach as described previously [30]. The microwell layout was designed using SolidWorks software (Solid Solutions Management Ltd, Dublin, Ireland). Moulds were designed with 100 microwells (10 × 10 array) containing 500 μm hemispherical concave microwells, with 1390 μm centre–centre distance and a depth of 1750 μm (Figure 1). A Formlabs Form 2 printer (Formlabs GmbH, Berlin, Germany) was used to 3D print the clear resin master stamps. After printing, the master stamps were washed in isopropyl alcohol for 20 min to remove excess residue and subsequently cured under an ultraviolet lamp (4 W, Uvitec, Cambridge, UK) for 1 h. 3D printed stamps were inserted into 12-well plates containing approximately 1 mL of PDMS (Sylgard® 184, Sigma-Aldrich, Arklow, Ireland), degassed in a

vacuum oven and cured at 80 °C for 4 h. After cooling, the master stamps were removed carefully with the use of a tweezers. The PDMS microwell moulds formed were washed with ethanol and phosphate-buffered saline (PBS, pH 7.4), sterilised by UV-irradiation for 3 h and allowed to dry overnight in a laminar hood. The morphology and the diameter of the PDMS microwells formed were characterised by scanning electron microscopy (SEM) (SEM, SUPRA 35 V P, Carl Zeiss, Oberkochen, Germany). For microtissue formation, the moulds were placed in 12-well plates and seeded with different densities of NP and NC cells (1000, 2500, and 5000 cells/microwell or 100,000, 250,000, 500,000 cells/mould) and centrifuged at $300\times g$ for 3 min to initiate microtissue formation. The plates were then cultured in a humified atmosphere at 37 °C and 5 %O_2 in 1 mL of media supplemented with or without growth factors as described below. Preliminary experiments investigated the formation of microtissues with less than 1000 cells/microtissue. However, these were found to be inconsistent and lacked cohesion and integrity, making them unsuitable for further experiments.

2.3. Growth Factor Stimulation

Microtissues were cultured in 1 mL of LG-DMEM with PenStrep, 1.5 mg/mL bovine serum albumin (BSA; Sigma-Aldrich), 1× insulin-transferrin-sodium selenite (ITS; Sigma-Aldrich), 40 µg/mL L-proline, 100 nM Dexamethasone, 50 µg/mL L-ascorbic acid 2-phosphate, 4.7 µg/mL linoleic acid and were either supplemented with no growth factor (control) or with 10 ng/mL TGFβ3 [31]. Microtissues were maintained at 37 °C for 7 days under low oxygen (5 %O_2) conditions. After 7 days of culture, microtissue size was evaluated through image analysis using Image J software (NIH, Bethesda, MA, USA). Initial results showed that lower cell density microtissues (1000 cells/microtissue) resulted in higher matrix production. Hence, this cell density was chosen for further experiments and they were individually supplemented with either 100 ng/mL of GDF5, 100 ng/mL of GDF6 [28], 10 ng/mL TGFβ3 + 100 ng/mL GDF5, 10 ng/mL TGFβ3 + 100 ng/mL GDF6 or 10 ng/mL TGFβ3 + 100 ng/mL GDF5 + 100 ng/mL GDF6.

2.4. In-Silico Modelling of Microtissue Nutrient Microenvironment

The in silico nutrient model of microtissues was created using COMSOL Multiphysics 5.6 (COMSOL Ltd., Cambridge, UK). Oxygen concentration at the microtissue boundary was dependent on multiple local environmental factors such as external level at the air/media interface, diffusion rate within the media, and the volume of media used. Glucose concentration and pH level at the microtissue boundary was dependent on the initial concentration of the media

and the volume of media. Therefore, the in silico model was based on the in vitro geometry of the media-filled microwell containing an idealised radially symmetric microtissue with an initial cell seeding density of 1000, 2500 or 5000 cells. Since oxygen kinetics occur on a faster timescale than cell cycle kinetics the radius of the microtissue was assumed to be constant. The steady-state nutrient microenvironment was governed by coupled reaction-diffusion equations as described previously for disc cells [32]. Briefly, the metabolic rates were modelled as being dependent on local oxygen and pH levels by employing Michaelis–Menten equations derived and published previously [32-35]. Results for oxygen, glucose and pH levels were predicted and displayed as concentration contour plots through the midplane of the microtissues and graphically as a function of normalised radial distance through the microtissues.

2.5. Live/Dead Analysis

Cell viability was assessed using the LIVE/DEAD® viability/cytotoxicity assay kit (Invitrogen, Biosciences, Dublin, Ireland). Briefly, microtissues were washed with PBS and incubated in live/dead solution containing 2 μM calcein AM (live cell membrane, abs/em = 494/517 nm) and 4 μM ethidium homodimer-1 (dead cell DNA, ex/em = 528/617 nm; both from Cambridge Bioscience, Cambridge, UK) in PBS for 1 h. Samples were then washed in PBS, imaged with a Leica SP8 scanning confocal microscope at 515 and 615 nm channels and assessed using Leica Application Suite X (LAS X) Software (Version 3.5.5.19976)

2.6. Quantitative Biochemical Analysis

After 7 days in culture, microtissues were flushed from the moulds with PBS and frozen at −80 °C for further analysis. Microtissues were digested with 3.88 U/mL papain in 0.1 M sodium acetate, 5 mM L-cysteine-HCl and 0.05 M ethylenediaminetetraacetic acid (EDTA) (pH 6.0) (all from Sigma-Aldrich) at 60 °C under constant rotation for 18 h. DNA content was quantified using the Quant-iT PicoGreen® dsDNA (Invitrogen) assay. sGAG content was quantified using the dimethylmethylene blue dye-binding assay at pH 1.35 (Blyscan, Biocolor Ltd., Carrickfergus, Northern Ireland), with a chondroitin sulphate standard. Total collagen content was determined by measuring the hydroxyproline content. Samples were hydrolysed at 110 °C for 18 h in 12 M HCl, assayed using a chloramine-T assay [36] and the collagen content determined using a hydroxyproline:collagen ratio of 1:7.69. Samples of media supernatants were also analysed for both sGAG and collagen content. DNA and sGAG contents were normalised based on the mass of all the microtissues (~100) from the entire microwell. The sGAG/collagen ratio was determined by dividing sGAG (μg) by collagen (μg).

2.7. Histology and Immunohistochemistry

Microtissues were treated with 4% paraformaldehyde (4 °C, 12 h) and washed in PBS. Microtissues were encapsulated in 2% agarose (Sigma-Aldrich) to facilitate handling, transferred to a cassette, dehydrated in a series of graded alcohols and finally wax embedded. Sections of 5 µm were stained with 1% alcian blue 8GX in 0.1 M HCl to assess sGAG deposition and with picrosirius red to evaluate collagen distribution. Collagen types I and II were assessed using immunohistochemistry techniques. Sections were treated with chondroitinase ABC (37 °C, 1 h) (Sigma-Aldrich), and non-specific sites were blocked using 5% BSA. Sections were incubated at 4 °C overnight with collagen type I (Abcam, Cambridge, UK) or collagen type II (Santa Cruz, Heidelberg, Germany) primary antibodies. The secondary antibody (Anti-Mouse igG biotin conjugate, Sigma-Aldrich) was applied for 1 h followed by incubation (45 min) with ABC reagent (Vectastain PK-400, Vector Labs, 2BScientific Ltd, Oxfordshire, UK). DAB peroxidase (Vector Labs, UK) was used as a developer.

2.8. Statistical Analysis

Statistical analysis was performed using GraphPad Prism (version 9.3.1, GraphPad Software, San Diego, CA, USA) software with 3–4 samples analysed for each experimental group. Two-way ANOVA was used for analysis of variance with Tukey's multiple comparisons test to compare between groups. Three technical replicates from three different porcine donors (biological replicates) were analysed. Results are displayed as mean ± standard deviation, with significance accepted at a level of $p < 0.05$.

3. Results

3.1. Design and Fabrication of PDMS Microwells

The master stamp prototype designed using SolidWorks software (Figure 1A) was fabricated using a Form 2 printer (Figure 1B). The printed stamps had a smooth and clear surface and were used to form the negative PDMS moulds. The PDMS moulds formed had 100 microwells (10×10 array) with 500 µm hemispherical concave microwells, with 1390 µm centre-centre distance and depth of 1750 µm (Figure 1C). The microwells had a uniform size with an average diameter of 504 ± 24 µm based on SEM images (Figure 1D).
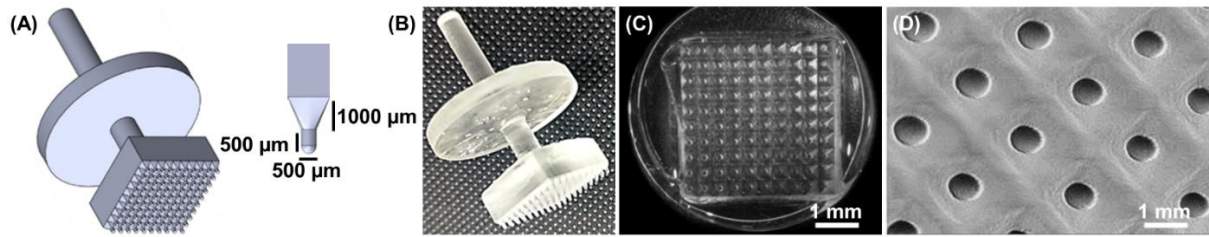
Figure 1. Fabrication of PDMS microwells for microtissue formation. (**A**) Design of the master stamp with negative pattern containing 10×10 microwells and the dimensions of the individual microwell. (**B**) 3D printed master stamp. (**C**) PDMS moulds with a 10×10 array for microtissue culture. (**D**) Microwells exhibited uniformity in size and shape as confirmed by SEM imaging.

3.2. Morphology and Viability of Microtissues

In terms of cell viability, results revealed high viability in low cell density microtissues with more dead cells being detected in the microtissues formed using higher cell numbers (Figure 2A). Moreover, the microtissues in the control group were loosely packed, exhibiting an irregular surface with loose arrangement of cells at the peripheral layers while the microtissues formed in the presence of TGFβ3 exhibited a smooth surface with compact organisation of the interior cells. The low cell density microtissues in the control group were also easily dissociated during the flushing process. The size of the microtissues increased with increasing cell numbers in both control and TGFβ3 treated groups for both NP and NC microtissues (Figure 2B). As expected, DNA content increased with higher content observed in higher cell density microtissues. NC microtissues exhibited increased DNA content (which indicates higher cell content) compared to NP microtissues, with a significant difference observed for 2500 and 5000 cells/microtissue cultured in the presence of TGFβ3 (Figure 2C).
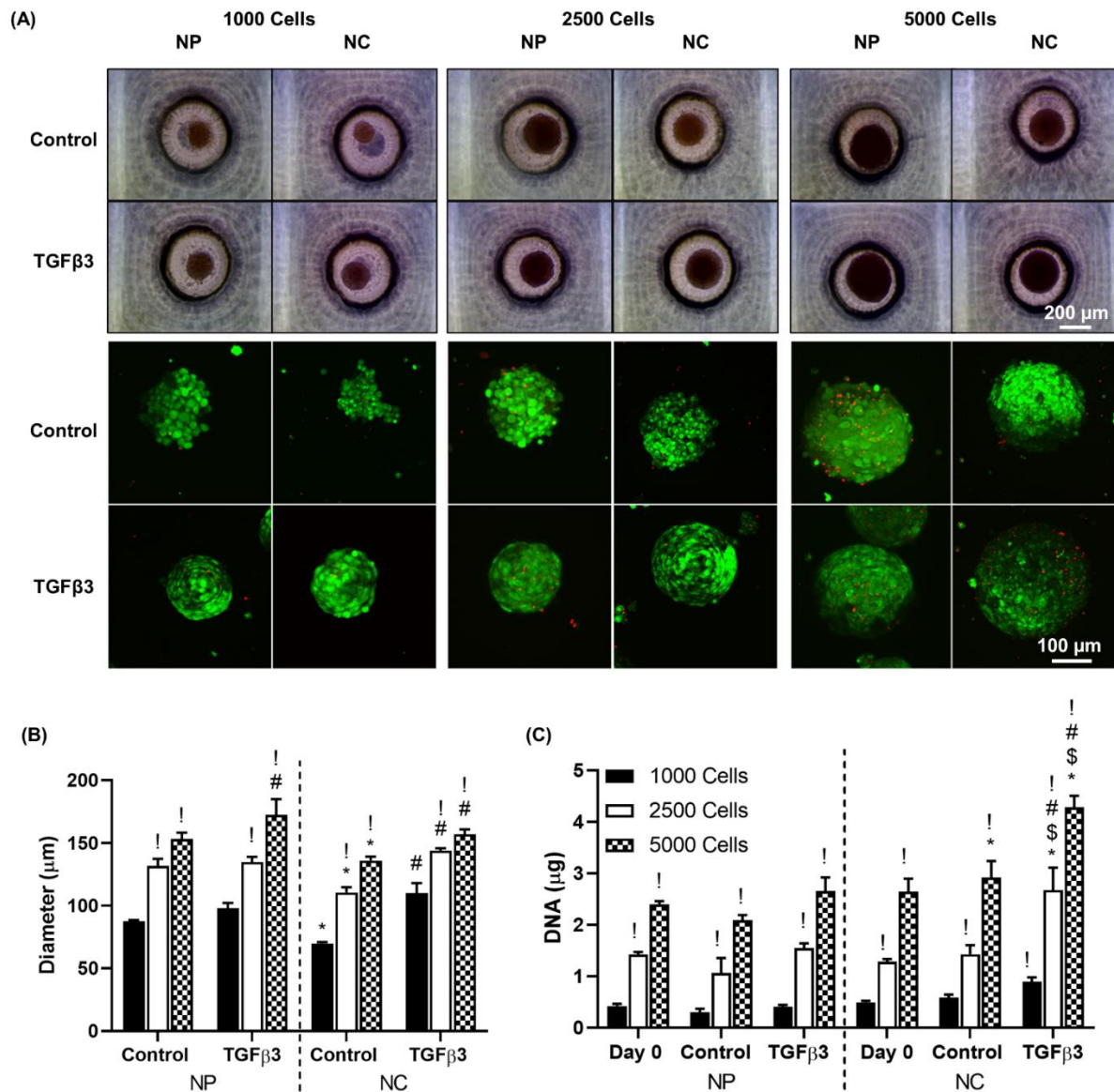
Figure 2. Morphology and viability of microtissues formed using nucleus pulposus (NP) and nasoseptal chondrocyte (NC) cells. (**A**) Representative brightfield and fluorescent Live/Dead® images demonstrating the morphology and viability of microtissues in microwells seeded with 1000, 2500 and 5000 cells/microwell, after 7 days (**B**) Diameter of microtissues were analysed using ImageJ (**C**) DNA content (µg) was determined in digested microtissues from moulds at each timepoint (day 0 or day 7). Data represent mean ± SD of at least three independent experiments performed in triplicate. ! ($p < 0.05$) indicates significance compared to 1000 cells/microtissue. # ($p < 0.05$) indicates significance compared to the control group for the same cell number. $ ($p < 0.05$) indicates significance compared to day 0 for the same cell number. * ($p < 0.05$) indicates significance compared to the NP microtissues for the same experimental group and cell number.

3.3. ECM Synthesis and Optimising Cell Density of TGFβ3 Stimulated Microtissues

Total sGAG content increased with increasing cell densities, with NC microtissues achieving significantly higher sGAG levels for all cell densities compared to NP microtissues cultured in the presence of TGFβ3 (Figure 3A). sGAG normalised to DNA showed increased sGAG/DNA for lower cell density microtissues and the NC 1000 cells/microtissue in TGFβ3 achieved a significantly higher level compared to NP 1000 cells/microtissue (Figure 3B). A similar trend was observed for total collagen content with higher cell density microtissues resulting in higher collagen accumulation (Figure 3C). Interestingly, when normalised to DNA content, NP 1000 cells/microtissue in TGFβ3 was significantly higher compared to NC 1000 cells/microtissue in TGFβ3 (Figure 3D). Strong alcian blue staining in lower cell density NC microtissues in TGFβ3 confirmed the higher synthesis of sGAG (Figure 3E). Picrosirius red staining for collagen also corroborated the collagen biochemical data with dense staining observed in NP 1000 cells/microtissue supplemented with TGFβ3. Comparatively, low cell density microtissues resulted in better ECM synthesis on a per cell basis and in silico modelling was performed to determine the nutrient microenvironment within the microwells to elucidate how this may be influencing matrix synthesis.
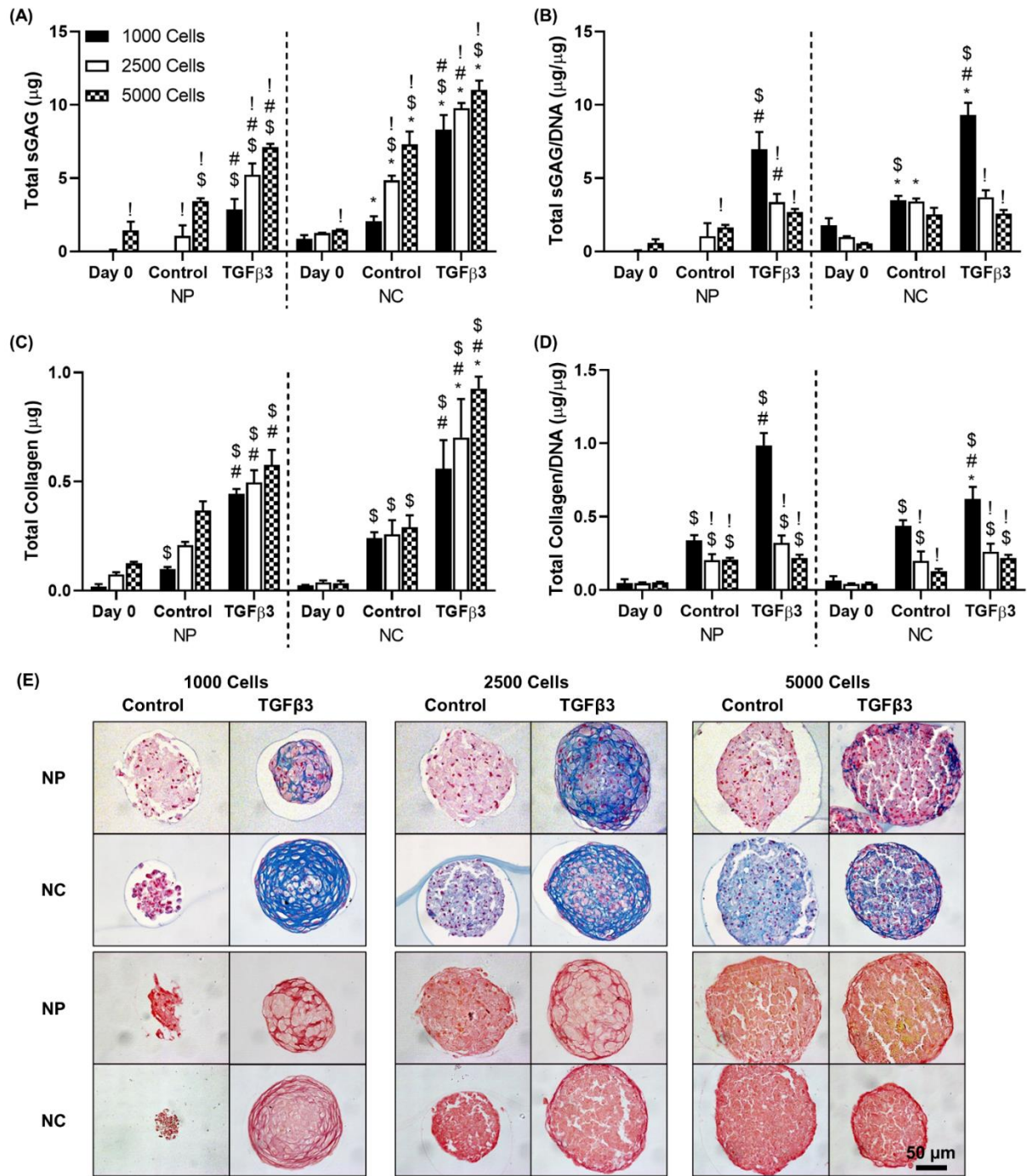
Figure 3. Biochemical and histological staining for sGAG and collagen of nucleus pulposus (NP) and nasoseptal chondrocyte (NC) microtissues stimulated with TGFβ3 on day 7. (**A**) Total sGAG (µg) content (**B**) Total sGAG/DNA (**C**) Total Collagen (µg) (**D**) Total Collagen/DNA. Data represent mean ± SD of at least three independent experiments performed in triplicate. ! ($p < 0.05$) indicates significance compared to 1000 cells/microtissue. # ($p < 0.05$) indicates significance compared to the control for the same cell number on day 7. $ ($p < 0.05$) indicates significance compared to day 0 for the same cell number. * ($p < 0.05$) indicates significance

compared to the NP microtissues for the same experimental group and cell number. (**E**) Histological evaluation with alcian blue staining and picrosirius red to identify sGAG collagen content, respectively.

3.4. In-Silico Modelling of Microtissue Nutrient Microenvironment

An in silico modelling analysis was performed based on the size of the microtissues for each of the cell densities investigated. As expected, an inverse relationship between metabolite concentration and cell density was observed and correlated well with the biochemical observations, whereby higher ECM on a per cell basis was observed with higher oxygen, glucose and pH levels. In terms of oxygen, minimum levels of 2.7 %O_2, 1.8 %O_2 and 0.9 %O_2 for 1000, 2500 and 5000 cells/microwell were observed, respectively (Figure 4A,B). For glucose, minimum levels of 4.6 mM, 4.1 mM and 3.4 mM (Figure 4C,D) and for pH, 7.3, 7.2 and 7.0 were observed for 1000, 2500 and 5000 cells/microwell respectively (Figure 4E,F). Minimal gradient effects from the centre to the periphery of microtissues were observed.
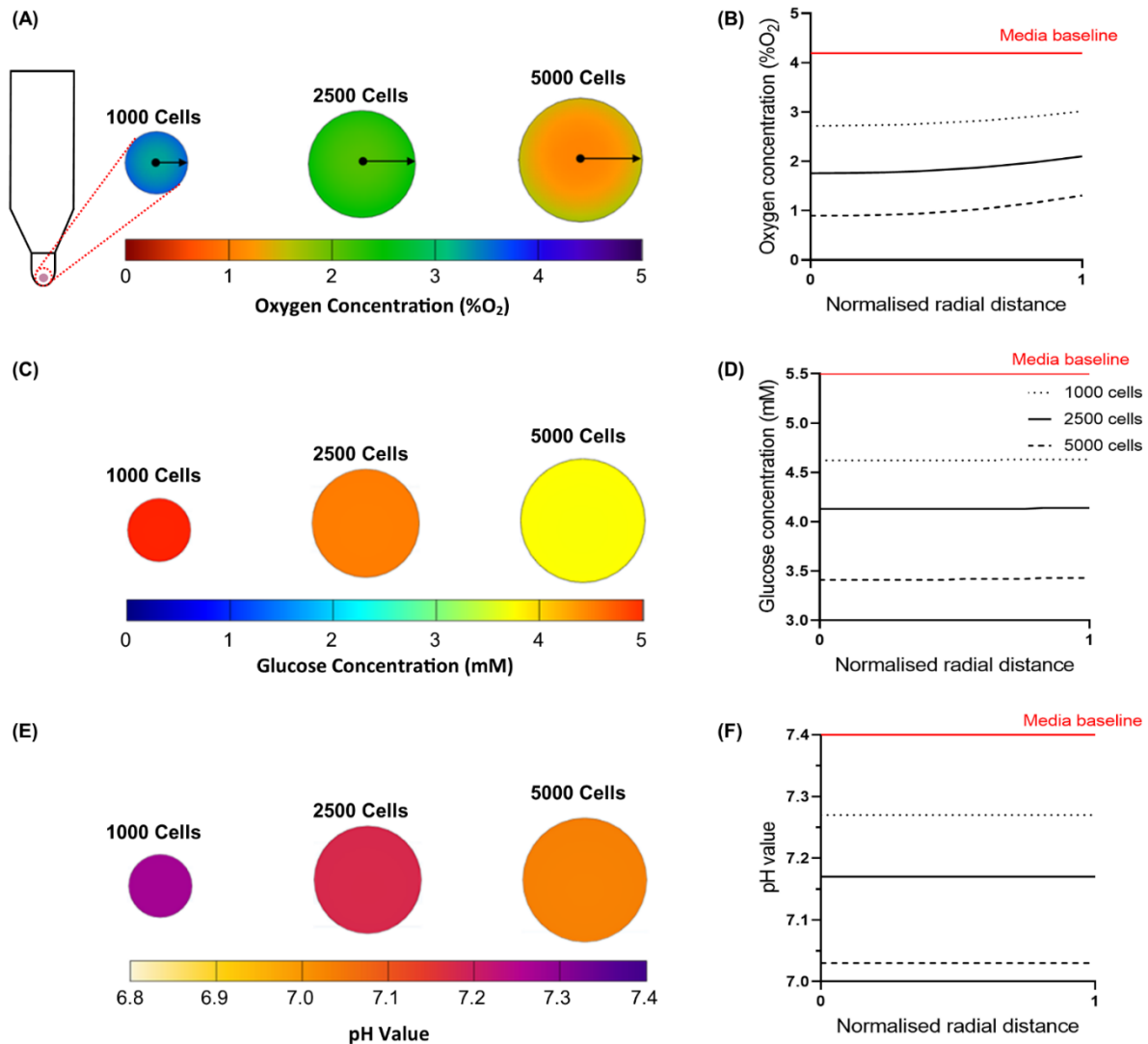
Figure 4. In silico modelling of the nutrient microenvironment within microtissues as a function of cell density. Predicted contour plots and radial profile through the midplane containing 1000, 2500 and 5000 cells for (**A,B**) oxygen (%O$_2$) (**C,D**) glucose (mM) and (**E,F**) pH. The radial distance was normalised by the radius of the microtissue for each cell density.

3.5. Viability and ECM Synthesis of Microtissues in the Presence of Different Growth Factors and Combinations

Based on the observations of lower cell density microtissues resulting in higher cell viability and matrix production, a cell density of 1000 cells/microtissue was chosen for further experiments. Microtissues formed by NCs were more compact compared to NP microtissues. No significant difference in viability was observed among the microtissues cultured in the presence of various growth factors, with high cell viability observed on day 7 (Figure 5A). Weak alcian blue staining for sGAG was observed in NP microtissues supplemented with GDF5 and

GDF6 growth factors in isolation. Increased positive staining was observed by co-stimulation with TGFβ3. For NC microtissues, GDF5 had a positive effect with minimal staining observed for GDF6. TGFβ3 co-stimulation resulted in intense staining and was comparatively stronger than NP microtissues (Figure 5B). Both NP and NC microtissues stained positive for collagen in the presence of GDF5, with higher deposition of collagen observed in the presence of GDF6 and when co-stimulated with TGFβ3 (Figure 5C).
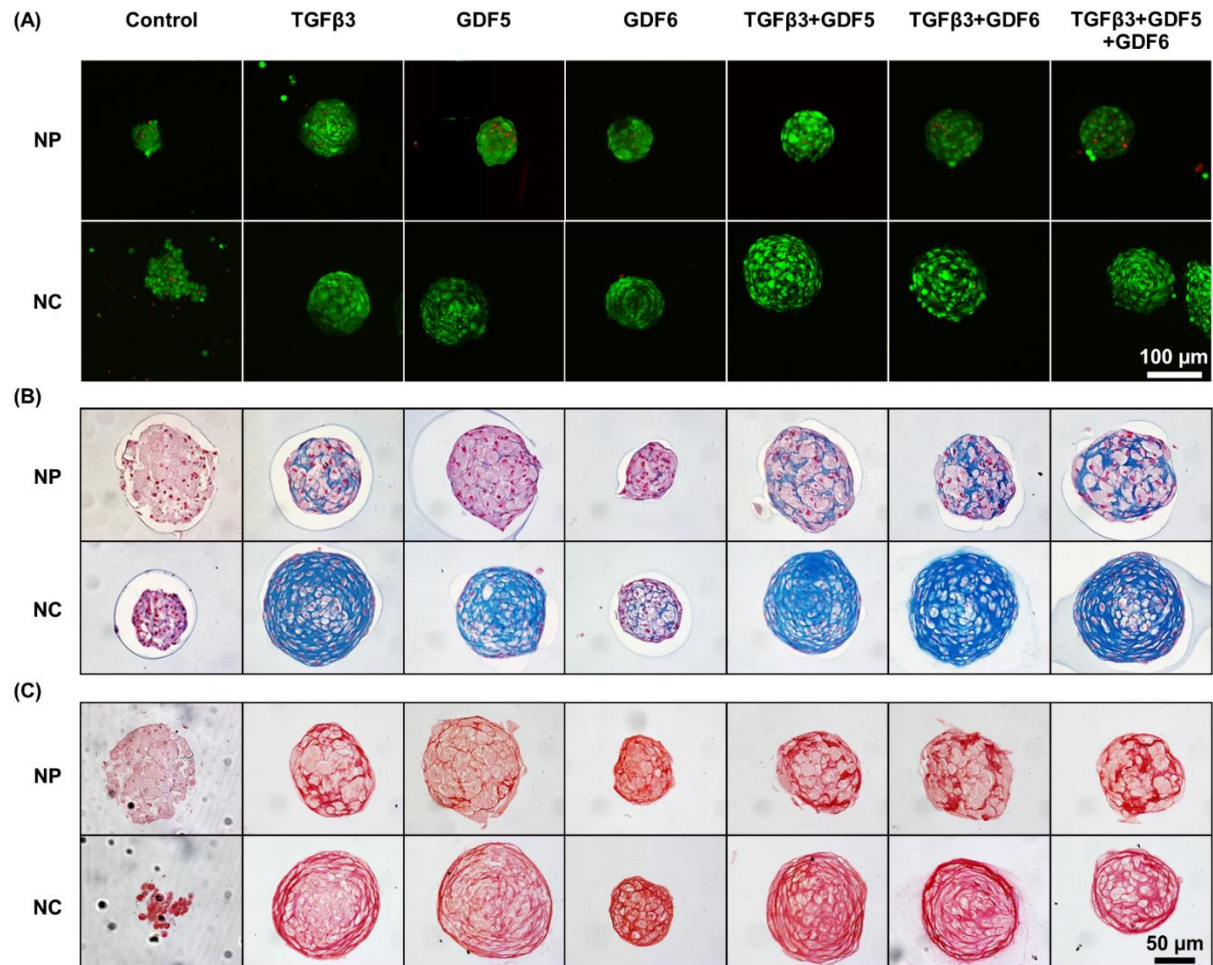

Figure 5. Live/Dead® and histological staining of nucleus pulposus (NP) and nasoseptal chondrocyte (NC) microtissues (1000 cells/microtissue) treated with no growth factor (control) or stimulated with TGFβ3, GDF5, GDF6, TGFβ3 + GDF5, TGFβ3 + GDF6, TGFβ3 + GDF5 + GDF6 on day 7. (**A**) Live/Dead® fluorescent images demonstrating cell viability. Histological evaluation with (**B**) alcian blue staining to identify sGAG and (**C**) picrosirius red to detect collagen.

3.6. Quantitative Biochemical Analysis of Microtissues in the Presence of Different Growth Factors

Both cell types responded positively to growth factor treatment relative to the no growth factor control (red solid line). For NP microtissues, no significant differences in DNA content were observed after 7 days irrespective of the growth factor type or combination. In contrast, a higher DNA content was observed in NC microtissues when cultured in the presence of GDF5 and all other combinations of growth factors relative to GDF6 (Figure 6A). Total sGAG was highest in NP microtissues stimulated with TGFβ3 + GDF5, although there were no significant differences between the groups investigated. Total sGAG levels in the NC microtissues were similar for all growth factor groups and combinations and were significantly higher compared to GDF6. Overall, sGAG levels for NC microtissues were significantly higher compared to NP microtissues (Figure 6B). When normalised by DNA content (sGAG/DNA), no differences were found between growth factor groups for a specific cell type, although NC microtissues still exhibited higher content compared to NP cells (Figure 6C).

In terms of total collagen content, for NP microtissues, a synergistic effect was observed through co-stimulation of growth factors (TGFβ3 + GDF5, TGFβ3 + GDF6 and TGFβ3 + GDF5 + GDF6) when compared to GDF5 and GDF6 alone. A similar synergistic effect was observed for NC microtissues when cultured in the presence of TGFβ3 + GDF5. However, the collagen content in NC microtissues treated with TGFβ3 + GDF6 and TGFβ3 + GDF5 + GDF6 were significantly higher than those treated with GDF5 alone. NC microtissues cultured in the presence of GDF6, TGFβ3 + GDF5 and TGFβ3 + GDF5 + GDF6 exhibited significantly higher collagen content compared to NP microtissues exposed to similar conditions (Figure 6D). Total collagen/DNA was significantly higher in NP microtissues cultured in the presence of TGFβ3 + GDF6, and no significant difference was observed when compared to TGFβ3 (red dashed line). However, for NC microtissues, GDF6-treated groups exhibited significantly higher concentrations compared to TGFβ3 (red dashed line), GDF5 and TGFβ3 + GDF5 + GDF6 treated groups (Figure 6E). In terms of sGAG/collagen level, which is a surrogate measure of NP-like matrix, with a higher ratio being desirable, no significant difference—irrespective of the growth factor treatment—was observed for NP microtissues. NC microtissues treated with GDF5 showed significantly higher concentrations compared to GDF6, TGFβ3 + GDF5 and TGFβ3 + GDF6. They also exhibited higher ratios compared to NP microtissues when cultured in the presence of TGFβ3 (red dashed line), GDF5, TGFβ3 + GDF5, TGFβ3 + GDF6 and TGFβ3 + GDF5 + GDF6 growth factor combinations (Figure 6F).
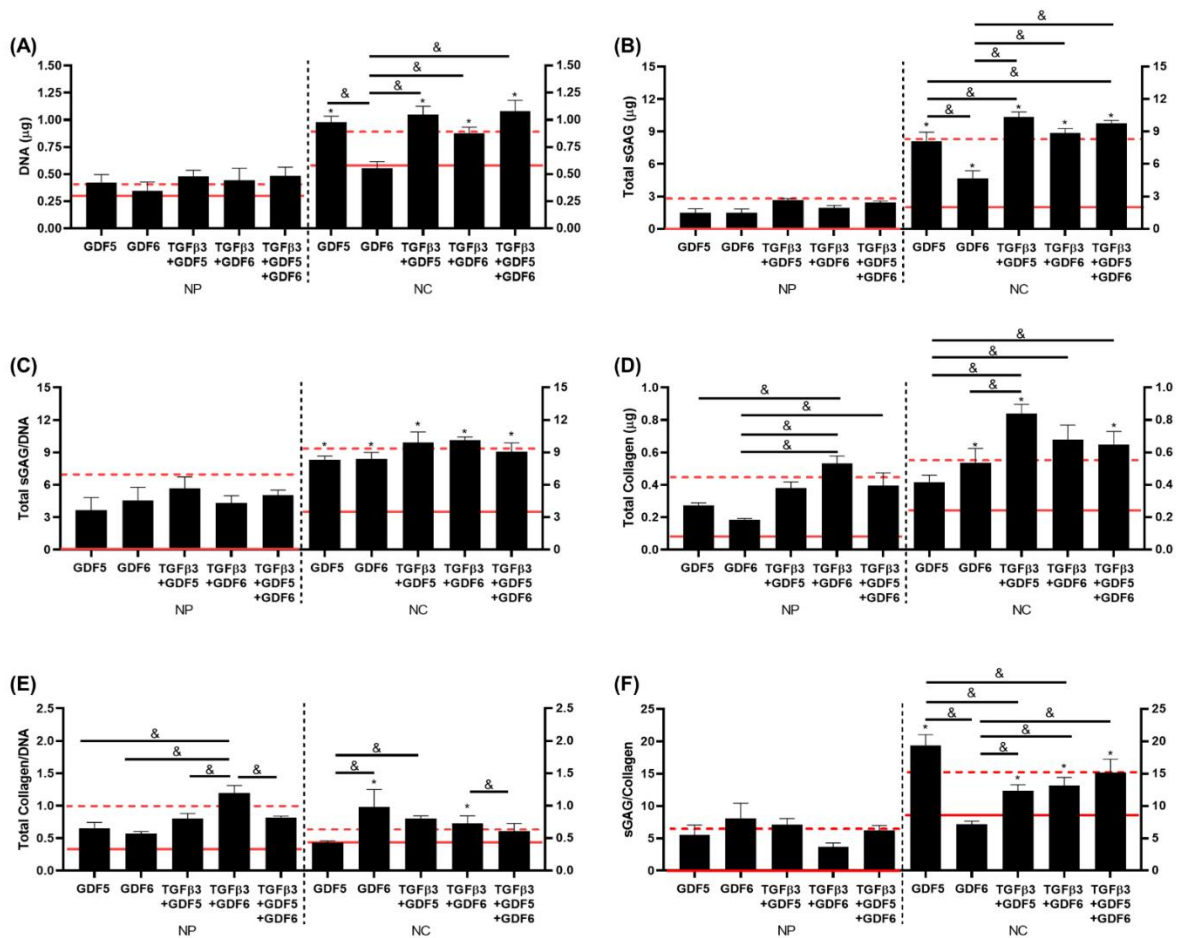
Figure 6. Biochemical analysis of nucleus pulposus (NP) and nasoseptal chondrocyte (NC) microtissues stimulated with GDF5, GDF6, TGFβ3 + GDF5, TGFβ3 + GDF6, TGFβ3 + GDF5 + GDF6 on day 7. (**A**) DNA (µg), (**B**) Total sGAG (µg), (**C**) Total sGAG/DNA, (**D**) Total Collagen (µg), (**E**) Total Collagen/DNA and (**F**) sGAG/Collagen ratio. & ($p < 0.05$) indicates significance compared to other growth factors in the same experimental group, * ($p < 0.05$) indicates significance compared to the NP microtissues for the same growth factor group. Solid red line indicates no growth factor treatment group (control); red dashed line indicates TGFβ3 stimulation group.

3.7. Immunostaining for Collagen Type of Microtissues in the Presence of Different Growth Factors

Irrespective of the growth factor used, immunostaining showed limited presence of collagen type I in both NP and NC microtissues (Figure 7A). NP microtissues also showed weak positive staining for collagen type II while NC microtissues stimulated with TGFβ3, GDF5 and TGFβ3 + GDF5 growth factors had higher and more dispersed collagen type II content (Figure 7B).
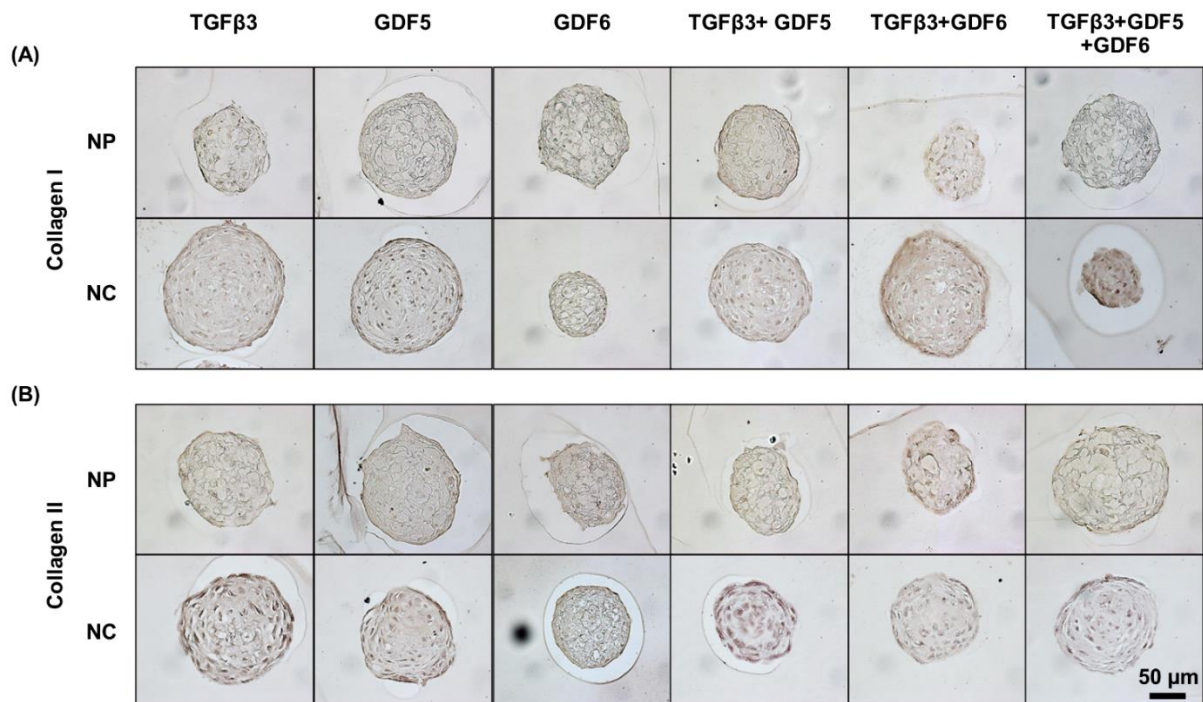
Figure 7. Immunostaining for collagen types I and II of nucleus pulposus (NP) and nasoseptal chondrocyte (NC) microtissues stimulated with TGFβ3, GDF5, GDF6, TGFβ3 + GDF5, TGFβ3 + GDF6, TGFβ3 + GDF5 + GDF6 on day 7. (**A**) Collagen type I and (**B**) Collagen type II.

4. Discussion

In this study, a microwell array system was used to promote the formation of self-assembled homogenous microtissues using two different cell types, nucleus pulposus cells and nasoseptal chondrocytes, and were subsequently assessed in response to growth factor stimulation. Growth factors TGFβ3, GDF5, GDF6 and a combination of these growth factors were assessed for their ability to induce matrix synthesis. The choice of growth factors selected was based on previous research in the field. For example, TGFβ3 is known to support the maintenance of the phenotype of disc cells in a rat lumbar organ culture [19] and MSCs supplemented with TGFβ3 support their differentiation towards an NP-like phenotype [37]. In addition, murine IVD explants treated exogenously with TGFβ3 have been shown to result in an up-regulation of aggrecan [38]. Studies have also shown that cells primed with TGFβ3 promoted higher sGAG and collagen synthesis [31,39] and also mitigated the detrimental effect of the harsh acidic microenvironment [40]. GDF5 (also known as cartilage-derived morphogenetic protein, CDMP1) and GDF6 (CDMP2) are members of the bone morphogenetic protein (BMP) family and are key regulators of cellular condensation and chondrogenesis [41]. GDF5 binds with

higher affinity to BMP receptor type-1B (BMPR-IB), which controls the primary stages of cellular condensation and promotes cartilaginous tissue formation [42,43]. GDF6 has been shown to promote chondrogenesis and it positively regulates growth and maintenance of articular cartilage [44]. Both GDF5 and GDF6 have been shown to induce the expression of NP associated genes in MSCs and adipose-derived stem cells (ASCs) [45] with a healthy NP phenotype exhibiting stabilised expression of hypoxia inducible factor HIF-1α, the glucose transporter glut-1, the PG aggrecan (ACAN), type II collagen (COL2A), the signalling factor sonic hedgehog (SHH), the transcription factor Brachyury [T], keratins KRT18, KRT19, carbonic anhydrase CA12, and CD24 [46].

We selected the growth factor concentrations of TGFβ3, GDF5, and GDF6, based on previous work stimulating bone marrow-derived MSCs and adipose-derived stem cells (ADSCs) which reported optimal expression of genes COL2 and ACAN when stimulated with 10 ng/mL TGFβ3 and 100 ng/mL GDF5 and GDF6 [28].

This study confirms that the initial cell seeding density of microtissues plays an important role in regulating ECM deposition. Although the amount of sGAG and collagen produced were highest in high cell density microtissues, sGAG and collagen synthesised on a per cell basis (per DNA) were highest in low density microtissues (1000 cells/microtissues). Based on the in silico models, higher cell density microtissues experienced lower nutrient levels and this in turn could alter the metabolism of the cells [32,47], and inhibit or impede matrix synthesis [39,48]. Overall, higher levels of matrix synthesis were observed for NC microtissues compared to NP microtissues, and it was significantly pronounced for NC microtissues stimulated with GDF5 or in combination with TGFβ3. In agreement with previous studies, microtissues stimulated with TGFβ3 resulted in increased proteoglycan synthesis compared to the controls [49,50]. TGFβ3 is widely known to modulate cell proliferation, differentiation and ECM synthesis and in particular supports chondrogenic differentiation of various cell types including mesenchymal stem cells [37,51-54], through the activation of the Wnt signalling pathway [55,56]. It has also been reported that Smad2/3 cooperatively is one of the important signalling pathways stimulated by TGFβ3 that helps in developing and maintaining a chondrocytic phenotype [57].

Given that increased ECM synthesis was observed in low cell density microtissues, we next explored the effect of growth factors—GDF5, GDF6 in isolation or in combination with TGFβ3. A synergistic effect on DNA content (indicative of increased cell number), total sGAG and total collagen was observed for both cell types with higher values observed in groups stimulated with the addition of TGFβ3 to GDF5 or GDF6, and this was evident for both cell types.

NP microtissues stimulated with TGFβ3 + GDF5 or TGFβ3 + GDF6 or TGFβ3 + GDF5 + GDF6 were comparable to TGFβ3 alone while the NC microtissues cultured in the presence of GDF5 alone were equally effective to TGFβ3 and had a synergistic effect when combined (TGFβ3 + GDF5). When these effects were evaluated on a per cell basis, the effects were diminished, with only a marginal increase observed in microtissues that were co-stimulated with growth factors. This was evident in the NC microtissues, but was not explicit in NP microtissues. Interestingly, Coleman et al. showed that MSCs co-stimulated with TGFβ3 (10 ng/mL) and GDF5 (150 ng/mL) resulted in a significant increase in sGAG/DNA by day 7 compared to TGFβ3 alone [58]. In this study, microtissues cultured in the combination of those growth factors did not result in any significant increase in proteoglycan synthesis on a per cell basis compared to TGFβ3 alone, irrespective of the cell type. This could be due to the lower concentration of GDF5 used (100 ng/mL) or could be attributed to the difference in the cell type or culturing conditions with lower oxygen and glucose concentrations. Another study by Jenner et al. showed that GDF5 stimulation caused an increase in cell numbers but collagen/DNA was significantly high in MSC scaffolds treated with TGFβ1 compared to GDF5 [59]. This trend was also observed in this study for NC microtissues, whereby TGFβ3 stimulation resulted in a significant increase in collagen/DNA compared to GDF5 only.

This study showed that GDF6 alone had little effect on DNA content (an indicator of cell number) for both NP and NC microtissues. This is in agreement with Bobacz et al., who reported no increase in cell numbers when articular chondrocytes were cultured in GDF6-supplemented media [60]. Gulati et al. showed that GDF6 at a concentration of 400 ng/mL resulted in a significant increase in proteoglycan accumulation in NP cells compared to the non-treated controls [27]. Similar observations were made in this study with both NP and NC microtissues exhibiting significantly higher sGAG/DNA in the presence of GDF6 compared to the non-treated controls.

sGAG/collagen was quantified to estimate the potential of the microtissues stimulated with various growth factors to produce the appropriate matrix type normally found in the disc. A higher ratio of sGAG composition of the ECM in comparison to the collagenous matrix is a predominant characteristic of NP tissue [45]. While no significant differences were observed for NP microtissues irrespective of the growth factor used, supplementation of NC microtissues with GDF5 or TGFβ3 alone or with the combination of growth factors (TGFβ3 + GDF5 + GDF6) yielded a significantly higher concentration. This implies that GDF5 or TGFβ3 alone could produce similar effects to the combination of growth factors indicating their potential to induce NC microtissues to form an NP-like matrix.

Recent research has shown that a combination of TGFβ1 and GDF5 significantly enhanced glycosaminoglycan content of human-derived MSCs, suggesting that this combination is optimal for MSC to NP cell induction [61]. Clarke et al. previously investigated the effect of TGFβ3, GDF5 and GDF6 growth factors on the discogenic differentiation of bone marrow- and adipose-derived MSCs (AD-MSCs). After 14 days, they observed that GDF6 resulted in increased expression of NP phenotypic genes KRT8, 18, and 19, FOX1 and CAXII compared to either TGFβ3 or GDF5 alone in both cell types with greater effects observed for AD-MSCs. However, they did not evaluate the effects of combining the growth factors [28].

In this study, GDF6 resulted in a higher sGAG/collagen ratio in NP microtissues, although this was not found to be statistically significant. On the other hand, GDF5 stimulation resulted in the highest sGAG/collagen ratio in NC microtissues, which was significantly higher than GDF6, TGFβ3 + GDF5 and TGFβ3 + GDF6. Interestingly, TGFβ3-only stimulation had a comparable effect to combinations with GDF5/GDF6. For NP microtissues, TGFβ3 also had a similar effect to other growth factors used in isolation and in combination, thereby demonstrating the potency of TGFβ3 in promoting matrix synthesis. The differential effects induced by the different growth factors, despite all belonging to the TGFβ superfamily, could be due to the difference in the signalling pathways activated. TGFβ3 is recognised by receptor type II, which activates the SMAD 2/3 signalling pathway, while GDF5 and GDF6 utilise the BMP receptor II, which activates the SMAD 1/5/8 pathway [28,62]. Activation of these distinct pathways ultimately results in different downstream signals, which may explain the differential effects observed in this study.

There are several limitations associated with the present study worth highlighting. First, longer term evaluation beyond 7 days may result in larger differences in microtissue maturation. However, this study is valuable as it demonstrates that microtissues stimulated with growth factors can produce a significant amount of ECM in a short time frame of 7 days, which would be compatible with a priming or conditioning strategy prior to implantation in the challenging disc microenvironment. We have previously shown that bone marrow stem cells (BMSCs) respond to growth factor stimulation (TGFβ3) under acidic conditions typically found in the degenerated disc (pH 6.8) [63]. A growth factor supplementation strategy with any of the growth factors assessed in this work may also prove to be beneficial. In addition, we have previously demonstrated that priming of BMSCs, NP and chondrocyte tissues with growth factors prior to a challenge or insult, confers better protection against acidic conditions, possibly due to the ECM being produced during the priming phase, thereby providing a protective

niche [31,40,64]. In addition, further investigations on the gene expression profile of NCs would be valuable to identify whether typical NP markers are up-regulated.

5. Conclusions

In this study, we have developed and evaluated self-assembled microtissues stimulated with various growth factors and combinations. In general, while NP cells did respond to growth factor stimulation, NP cells were found to be relatively insensitive to the different growth factor types examined in isolation or in combination in this experimental setting. In contrast, NCs, which are more easily isolated in a less invasive manner and are more easily expandable, may prove to be an alternative cell type for NP repair and these cells could be primed with either GDF5 or TGFβ3 to enhance matrix synthesis.

References

1. Sakai, D.; Mochida, J.; Yamamoto, Y.; Nomura, T.; Okuma, M.; Nishimura, K.; Nakai, T.; Ando, K.; Hotta, T. Transplantation of mesenchymal stem cells embedded in Atelocollagen gel to the intervertebral disc: A potential therapeutic model for disc degeneration. *Biomaterials* **2003**, *24*, 3531–3541.

2. Zhang, Y.; Drapeau, S.; Howard, S.A.; Thonar, E.J.; Anderson, D.G. Transplantation of goat bone marrow stromal cells to the degenerating intervertebral disc in a goat disc injury model. *Spine* **2011**, *36*, 372–377. https://doi.org/10.1097/BRS.0b013e3181d10401.

3. Acosta, F.L., Jr.; Metz, L.; Adkisson, H.D.; Liu, J.; Carruthers-Liebenberg, E.; Milliman, C.; Maloney, M.; Lotz, J.C. Porcine intervertebral disc repair using allogeneic juvenile articular chondrocytes or mesenchymal stem cells. *Tissue Eng. Part A* **2011**, *17*, 3045–3055. https://doi.org/10.1089/ten.tea.2011.0229.

4. Lyu, F.J.; Cheung, K.M.; Zheng, Z.; Wang, H.; Sakai, D.; Leung, V.Y. IVD progenitor cells: A new horizon for understanding disc homeostasis and repair. *Nat. Rev. Rheumatol.* **2019**, *15*, 102–112. https://doi.org/10.1038/s41584-018-0154-x.

5. Meisel, H.J.; Siodla, V.; Ganey, T.; Minkus, Y.; Hutton, W.C.; Alasevic, O.J. Clinical experience in cell-based therapeutics: Disc chondrocyte transplantation A treatment for degenerated or damaged intervertebral disc. *Biomol. Eng.* **2007**, *24*, 5–21, doi:S1389-0344(06)00075-X [pii]10.1016/j.bioeng.2006.07.002.

6. Smith, L.J.; Silverman, L.; Sakai, D.; Le Maitre, C.L.; Mauck, R.L.; Malhotra, N.R.; Lotz, J.C.; Buckley, C.T. Advancing cell therapies for intervertebral disc regeneration from the lab to the clinic: Recommendations of the ORS spine section. *JOR Spine* **2018**, *1*, e1036. https://doi.org/10.1002/jsp2.1036.

7. Mochida, J.; Sakai, D.; Nakamura, Y.; Watanabe, T.; Yamamoto, Y.; Kato, S. Intervertebral disc repair with activated nucleus pulposus cell transplantation: A three-year, prospective clinical study of its safety. *Eur. Cells Mater.* **2015**, *29*, 202–212.

8. Sakai, D.; Schol, J. Cell therapy for intervertebral disc repair: Clinical perspective. *J. Orthop. Transl.* **2017**, *9*, 8–18. https://doi.org/10.1016/j.jot.2017.02.002.

9. Benneker, L.M.; Andersson, G.; Iatridis, J.C.; Sakai, D.; Hartl, R.; Ito, K.; Grad, S. Cell therapy for intervertebral disc repair: Advancing cell therapy from bench to clinics. *Eur. Cells Mater.* **2014**, *27*, 5–11. https://doi.org/10.22203/ecm.v027sa02.

10. Vadala, G.; Sowa, G.; Hubert, M.; Gilbertson, L.G.; Denaro, V.; Kang, J.D. Mesenchymal stem cells injection in degenerated intervertebral disc: Cell leakage may induce osteophyte formation. *J. Tissue Eng. Regen. Med.* **2012**, *6*, 348–355. https://doi.org/10.1002/term.433.

11. Vedicherla, S.; Buckley, C.T. In vitro extracellular matrix accumulation of nasal and articular chondrocytes for intervertebral disc repair. *Tissue Cell* **2017**, *49*, 503–513. https://doi.org/10.1016/j.tice.2017.05.002.

12. Gay, M.H.; Mehrkens, A.; Rittmann, M.; Haug, M.; Barbero, A.; Martin, I.; Schaeren, S. Nose to back: Compatibility of nasal chondrocytes with environmental conditions mimicking a degenerated intervertebral disc. *Eur. Cells Mater.* **2019**, *37*, 214–232. https://doi.org/10.22203/eCM.v037a13.

13. Borrelli, C.; Buckley, C.T. Synergistic Effects of Acidic pH and Pro-Inflammatory Cytokines IL-1 beta and TNF-alpha for Cell-Based Intervertebral Disc Regeneration. *Appl. Sci.* **2020**, *10*, 9009. https://doi.org/10.3390/app10249009.

14. Rotter, N.; Bonassar, L.J.; Tobias, G.; Lebl, M.; Roy, A.K.; Vacanti, C.A. Age dependence of cellular properties of human septal cartilage: Implications for tissue engineering. *Arch. Otolaryngol. Head Neck Surg.* **2001**, *127*, 1248–1252.

15. Rotter, N.; Bonassar, L.J.; Tobias, G.; Lebl, M.; Roy, A.K.; Vacanti, C.A. Age dependence of biochemical and biomechanical properties of tissue-engineered human septal cartilage. *Biomaterials* **2002**, *23*, 3087–3094.

16. Pratsinis, H.; Kletsas, D. Growth factors in intervertebral disc homeostasis. *Connect. Tissue Res.* **2008**, *49*, 273–276. https://doi.org/10.1080/03008200802147951.

17. Chen, S.; Liu, S.; Ma, K.; Zhao, L.; Lin, H.; Shao, Z. TGF-beta signaling in intervertebral disc health and disease. *Osteoarthr. Cartil.* **2019**, *27*, 1109–1117. https://doi.org/10.1016/j.joca.2019.05.005.

18. Bian, Q.; Ma, L.; Jain, A.; Crane, J.L.; Kebaish, K.; Wan, M.; Zhang, Z.; Edward Guo, X.; Sponseller, P.D.; Seguin, C.A.; et al. Mechanosignaling activation of TGFbeta maintains intervertebral disc homeostasis. *Bone Res.* **2017**, *5*, 17008. https://doi.org/10.1038/boneres.2017.8.

19. Risbud, M.V.; Di Martino, A.; Guttapalli, A.; Seghatoleslami, R.; Denaro, V.; Vaccaro, A.R.; Albert, T.J.; Shapiro, I.M. Toward an optimum system for intervertebral disc organ culture: TGF-beta 3 enhances nucleus pulposus and anulus fibrosus survival and function through modulation of TGF-beta-R expression and ERK signaling. *Spine* **2006**, *31*, 884–890. https://doi.org/10.1097/01.brs.0000209335.57767.b5.

20. Kim, M.J.; Lee, J.H.; Kim, J.S.; Kim, H.Y.; Lee, H.C.; Byun, J.H.; Lee, J.H.; Kim, N.H.; Oh, S.H. Intervertebral Disc Regeneration Using Stem Cell/Growth Factor-Loaded Porous Particles with a Leaf-Stacked Structure. *Biomacromolecules* **2020**, *21*, 4795–4805. https://doi.org/10.1021/acs.biomac.0c00992.

21. Le Maitre, C.L.; Freemont, A.J.; Hoyland, J.A. Localization of degradative enzymes and their inhibitors in the degenerate human intervertebral disc. *J. Pathol.* **2004**, *204*, 47–54. https://doi.org/10.1002/path.1608.

22. Settle, S.H., Jr.; Rountree, R.B.; Sinha, A.; Thacker, A.; Higgins, K.; Kingsley, D.M. Multiple joint and skeletal patterning defects caused by single and double mutations in the mouse Gdf6 and Gdf5 genes. *Dev. Biol.* **2003**, *254*, 116–130. https://doi.org/10.1016/s0012-1606(02)00022-2.

23. Wolfman, N.M.; Hattersley, G.; Cox, K.; Celeste, A.J.; Nelson, R.; Yamaji, N.; Dube, J.L.; DiBlasio-Smith, E.; Nove, J.; Song, J.J.; et al. Ectopic induction of tendon and ligament in rats by growth and differentiation factors 5, 6, and 7, members of the TGF-beta gene family. *J. Clin. Invest.* **1997**, *100*, 321–330. https://doi.org/10.1172/JCI119537.

24. Enochson, L.; Stenberg, J.; Brittberg, M.; Lindahl, A. GDF5 reduces MMP13 expression in human chondrocytes via DKK1 mediated canonical Wnt signaling inhibition. *Osteoarthr. Cartil.* **2014**, *22*, 566–577. https://doi.org/10.1016/j.joca.2014.02.004.

25. Guo, S.; Cui, L.; Xiao, C.; Wang, C.; Zhu, B.; Liu, X.; Li, Y.; Liu, X.; Wang, D.; Li, S. The Mechanisms and Functions of GDF-5 in Intervertebral Disc Degeneration. *Orthop. Surg.* **2021**, *13*, 734–741. https://doi.org/10.1111/os.12942.

26. Risbud, M.V.; Shapiro, I.M. Role of cytokines in intervertebral disc degeneration: Pain and disc content. *Nat. Rev. Rheumatol.* **2014**, *10*, 44–56. https://doi.org/10.1038/nrrheum.2013.160.

27. Gulati, T.; Chung, S.A.; Wei, A.Q.; Diwan, A.D. Localization of bone morphogenetic protein 13 in human intervertebral disc and its molecular and functional effects in vitro in 3D culture. *J. Orthop. Res.* **2015**, *33*, 1769–1775. https://doi.org/10.1002/jor.22965.

28. Clarke, L.E.; McConnell, J.C.; Sherratt, M.J.; Derby, B.; Richardson, S.M.; Hoyland, J.A. Growth differentiation factor 6 and transforming growth factor-beta differentially mediate mesenchymal stem cell differentiation, composition, and micromechanical properties of nucleus pulposus constructs. *Arthritis Res.* **2014**, *16*, R67. https://doi.org/10.1186/ar4505.

29. Vedicherla, S.; Buckley, C.T. Rapid Chondrocyte Isolation for Tissue Engineering Applications: The Effect of Enzyme Concentration and Temporal Exposure on the Matrix Forming Capacity of Nasal Derived Chondrocytes. *BioMed Res. Int.* **2017**, *2017*, 2395138. https://doi.org/10.1155/2017/2395138.

30. Futrega, K.; Palmer, J.S.; Kinney, M.; Lott, W.B.; Ungrin, M.D.; Zandstra, P.W.; Doran, M.R. The microwell-mesh: A novel device and protocol for the high throughput manufacturing of cartilage microtissues. *Biomaterials* **2015**, *62*, 1–12. https://doi.org/10.1016/j.biomaterials.2015.05.013.

31. Naqvi, S.M.; Gansau, J.; Buckley, C.T. Priming and cryopreservation of microencapsulated marrow stromal cells as a strategy for intervertebral disc regeneration. *Biomed. Mater.* **2018**, *13*, 034106. https://doi.org/10.1088/1748-605X/aaab7f.

32. McDonnell, E.E.; Buckley, C.T. Investigating the physiological relevance of ex vivo disc organ culture nutrient microenvironments using in silico modeling and experimental validation. *JOR Spine* **2021**, 4, e1141. https://doi.org/10.1002/jsp2.1141.

33. Bibby, S.R.; Jones, D.A.; Ripley, R.M.; Urban, J.P. Metabolism of the intervertebral disc: Effects of low levels of oxygen, glucose, and pH on rates of energy metabolism of bovine nucleus pulposus cells. *Spine* **2005**, *30*, 487–496.

34. Huang, C.Y.; Yuan, T.Y.; Jackson, A.R.; Hazbun, L.; Fraker, C.; Gu, W.Y. Effects of low glucose concentrations on oxygen consumption rates of intervertebral disc cells. *Spine* **2007**, *32*, 2063–2069. https://doi.org/10.1097/BRS.0b013e318145a521.

35. Huang, C.Y.; Gu, W.Y. Effects of mechanical compression on metabolism and distribution of oxygen and lactate in intervertebral disc. *J Biomech* **2008**, *41*, 1184–1196. https://doi.org/10.1016/j.jbiomech.2008.02.002.

36. Kafienah, W.; Sims, T.J. Biochemical methods for the analysis of tissue-engineered cartilage. *Methods Mol. Biol.* **2004**, *238*, 217–230.

37. Gupta, M.S.; Cooper, E.S.; Nicoll, S.B. Transforming growth factor-beta 3 stimulates cartilage matrix elaboration by human marrow-derived stromal cells encapsulated in photocrosslinked carboxymethylcellulose hydrogels: Potential for nucleus pulposus replacement. *Tissue Eng. Part A* **2011**, *17*, 2903–2910. https://doi.org/10.1089/ten.TEA.2011.0152.

38. Pelle, D.W.; Peacock, J.D.; Schmidt, C.L.; Kampfschulte, K.; Scholten, D.J., 2nd; Russo, S.S.; Easton, K.J.; Steensma, M.R. Genetic and functional studies of the intervertebral disc: A novel murine intervertebral disc model. *PLoS ONE* **2014**, *9*, e112454. https://doi.org/10.1371/journal.pone.0112454.

39. Naqvi, S.M.; Buckley, C.T. Differential response of encapsulated nucleus pulposus and bone marrow stem cells in isolation and coculture in alginate and chitosan hydrogels. *Tissue Eng. Part A* **2015**, *21*, 288–299. https://doi.org/10.1089/ten.TEA.2013.0719.

40. Gansau, J.; Buckley, C.T. Priming as a strategy to overcome detrimental pH effects on cells for intervertebral disc regeneration. *Eur. Cells Mater.* **2021**, *41*, 153–169. https://doi.org/10.22203/eCM.v041a11.

41. Coleman, C.M.; Tuan, R.S. Functional role of growth/differentiation factor 5 in chondrogenesis of limb mesenchymal cells. *Mech. Dev.* **2003**, *120*, 823–836. https://doi.org/10.1016/s0925-4773(03)00067-4.

42. Nishitoh, H.; Ichijo, H.; Kimura, M.; Matsumoto, T.; Makishima, F.; Yamaguchi, A.; Yamashita, H.; Enomoto, S.; Miyazono, K. Identification of type I and type II serine/threonine kinase receptors for growth/differentiation factor-5. *J. Biol. Chem.* **1996**, *271*, 21345–21352. https://doi.org/10.1074/jbc.271.35.21345.

43. Zou, H.; Wieser, R.; Massague, J.; Niswander, L. Distinct roles of type I bone morphogenetic protein receptors in the formation and differentiation of cartilage. *Genes Dev.* **1997**, *11*, 2191–2203. https://doi.org/10.1101/gad.11.17.2191.

44. Gooch, K.J.; Blunk, T.; Courter, D.L.; Sieminski, A.L.; Vunjak-Novakovic, G.; Freed, L.E. Bone morphogenetic proteins-2, -12, and -13 modulate in vitro development of engineered cartilage. *Tissue Eng.* **2002**, *8*, 591–601. https://doi.org/10.1089/107632702760240517.

45. Hodgkinson, T.; Shen, B.; Diwan, A.; Hoyland, J.A.; Richardson, S.M. Therapeutic potential of growth differentiation factors in the treatment of degenerative disc diseases. *JOR Spine* **2019**, *2*, e1045. https://doi.org/10.1002/jsp2.1045.

46. Risbud, M.V.; Schoepflin, Z.R.; Mwale, F.; Kandel, R.A.; Grad, S.; Iatridis, J.C.; Sakai, D.; Hoyland, J.A. Defining the phenotype of young healthy nucleus pulposus cells: Recommendations of the Spine Research Interest Group at the 2014 annual ORS meeting. *J. Orthop. Res.* **2015**, *33*, 283–293. https://doi.org/10.1002/jor.22789.

47. Wen-tao, Q.; Ying, Z.; Juan, M.; Xin, G.; Yu-bing, X.; Wei, W.; Xiaojun, M. Optimization of the cell seeding density and modeling of cell growth and metabolism using the modified Gompertz model for microencapsulated animal cell culture. *Biotechnol. Bioeng.* **2006**, *93*, 887–895. https://doi.org/10.1002/bit.20782.

48. Foldager, C.B.; Gomoll, A.H.; Lind, M.; Spector, M. Cell Seeding Densities in Autologous Chondrocyte Implantation Techniques for Cartilage Repair. *Cartilage* **2012**, *3*, 108–117. https://doi.org/10.1177/1947603511435522.

49. Zamani, S.; Hashemibeni, B.; Esfandiari, E.; Kabiri, A.; Rabbani, H.; Abutorabi, R. Assessment of TGF-beta3 on production of aggrecan by human articular chondrocytes in pellet culture system. *Adv. Biomed. Res.* **2014**, *3*, 54. https://doi.org/10.4103/2277-9175.125799.

50. Chen, J.; Wang, Y.; Chen, C.; Lian, C.; Zhou, T.; Gao, B.; Wu, Z.; Xu, C. Exogenous Heparan Sulfate Enhances the TGF-beta3-Induced Chondrogenesis in Human Mesenchymal Stem Cells by Activating TGF-beta/Smad Signaling. *Stem. Cells Int.* **2016**, *2016*, 1520136. https://doi.org/10.1155/2016/1520136.

51. Byers, B.A.; Mauck, R.L.; Chiang, I.E.; Tuan, R.S. Transient exposure to transforming growth factor beta 3 under serum-free conditions enhances the biomechanical and biochemical maturation of tissue-engineered cartilage. *Tissue Eng. Part A* **2008**, *14*, 1821–1834. https://doi.org/10.1089/ten.tea.2007.0222.

52. Huang, A.H.; Stein, A.; Tuan, R.S.; Mauck, R.L. Transient exposure to transforming growth factor beta 3 improves the mechanical properties of mesenchymal stem cell-laden cartilage

constructs in a density-dependent manner. *Tissue Eng. Part A* **2009**, *15*, 3461–3472. https://doi.org/10.1089/ten.TEA.2009.0198.

53. Afizah, H.; Yang, Z.; Hui, J.H.; Ouyang, H.W.; Lee, E.H. A comparison between the chondrogenic potential of human bone marrow stem cells (BMSCs) and adipose-derived stem cells (ADSCs) taken from the same donors. *Tissue Eng.* **2007**, *13*, 659–666. https://doi.org/10.1089/ten.2006.0118.

54. Amin, H.D.; Brady, M.A.; St-Pierre, J.P.; Stevens, M.M.; Overby, D.R.; Ethier, C.R. Stimulation of chondrogenic differentiation of adult human bone marrow-derived stromal cells by a moderate-strength static magnetic field. *Tissue Eng. Part A* **2014**, *20*, 1612–1620. https://doi.org/10.1089/ten.tea.2013.0307.

55. Li, S.; Macon, A.L.B.; Jacquemin, M.; Stevens, M.M.; Jones, J.R. Sol-gel derived lithium-releasing glass for cartilage regeneration. *J. Biomater. Appl.* **2017**, *32*, 104–113. https://doi.org/10.1177/0885328217706640.

56. Li, D.; Ma, X.; Zhao, T. Mechanism of TGF-beta3 promoting chondrogenesis in human fat stem cells. *Biochem. Biophys. Res. Commun.* **2020**, *530*, 725–731. https://doi.org/10.1016/j.bbrc.2020.06.147.

57. Furumatsu, T.; Tsuda, M.; Taniguchi, N.; Tajima, Y.; Asahara, H. Smad3 induces chondrogenesis through the activation of SOX9 via CREB-binding protein/p300 recruitment. *J. Biol. Chem.* **2005**, *280*, 8343–8350. https://doi.org/10.1074/jbc.M413913200.

58. Coleman, C.M.; Vaughan, E.E.; Browe, D.C.; Mooney, E.; Howard, L.; Barry, F. Growth differentiation factor-5 enhances in vitro mesenchymal stromal cell chondrogenesis and hypertrophy. *Stem. Cells Dev.* **2013**, *22*, 1968–1976. https://doi.org/10.1089/scd.2012.0282.

59. Jenner, J.M.; van Eijk, F.; Saris, D.B.; Willems, W.J.; Dhert, W.J.; Creemers, L.B. Effect of transforming growth factor-beta and growth differentiation factor-5 on proliferation and matrix production by human bone marrow stromal cells cultured on braided poly lactic-co-glycolic acid scaffolds for ligament tissue engineering. *Tissue Eng.* **2007**, *13*, 1573–1582. https://doi.org/10.1089/ten.2006.0208.

60. Bobacz, K.; Gruber, R.; Soleiman, A.; Erlacher, L.; Smolen, J.S.; Graninger, W.B. Expression of bone morphogenetic protein 6 in healthy and osteoarthritic human articular chondrocytes and stimulation of matrix synthesis in vitro. *Arthritis Rheum.* **2003**, *48*, 2501–2508. https://doi.org/10.1002/art.11248.

61. Morita, K.; Schol, J.; Volleman, T.N.E.; Sakai, D.; Sato, M.; Watanabe, M. Screening for Growth-Factor Combinations Enabling Synergistic Differentiation of Human MSC to Nucleus Pulposus Cell-Like Cells. *Appl. Sci.* **2021**, *11*, 3673.

62. Mazerbourg, S.; Sangkuhl, K.; Luo, C.W.; Sudo, S.; Klein, C.; Hsueh, A.J. Identification of receptors and signaling pathways for orphan bone morphogenetic protein/growth differentiation factor ligands based on genomic analyses. *J. Biol. Chem.* **2005**, *280*, 32122–32132. https://doi.org/10.1074/jbc.M504629200.

63. Naqvi, S.M.; Buckley, C.T. Bone Marrow Stem Cells in Response to Intervertebral Disc-Like Matrix Acidity and Oxygen Concentration: Implications for Cell-based Regenerative Therapy. *Spine* **2016**, *41*, 743–750. https://doi.org/10.1097/brs.0000000000001314.

64. Naqvi, S.M.; Gansau, J.; Gibbons, D.; Buckley, C.T. In vitro co-culture and ex vivo organ culture assessment of primed and cryopreserved stromal cell microcapsules for IVD regeneration. *Eur. Cells Mater.* **2019**, *37*, 134–152. https:doi.org/10.22203/eCM.v037a09.